Crustal-scale transcurrent shearing in the Paleoproterozoic Sefwi-Sunyani-Comoé region, West Africa

Mark W. Jessell [a,b,*], Prince O. Amponsah [c], Lenka Baratoux [a,b], Daniel K. Asiedu [c], Geoffrey K. Loh [d], Jérôme Ganne [a,b]

[a] Université de Toulouse, GET, OMP, 14 Av. Edouard Belin, F-31400 Toulouse, France
[b] IRD, GET, F-31400 Toulouse, France
[c] Department of Geology, University of Ghana, PO Box LG 58, Legon, Accra, Ghana
[d] Geological Survey Department, PO Box M.80, Accra, Ghana

ARTICLE INFO

ABSTRACT

The Paleoproterozoic Sefwi-Sunyani-Comoé region that straddles the Ghana-Ivory Coast border in West Africa has been characterised as resulting from a combination of compression and simple shear with leucogranite intrusion either being prior to the compression or synchronous with late shearing. The analysis of regional magnetic datasets combined with field observations allows us to better define the geometry of the major lithostratigraphic packages and their structural contacts in this region. This analysis reveals a series of elongate rounded leucogranite intrusions enveloped by deformed metasediments.

Recent finite element modelling of two-phase aggregates has shown that we can analyse the geometry of these systems both in terms of their finite deformation and their mechanical contrast. We interpret the geometries we see in the Sefwi-Sunyani-Comoé region as reflecting the activity of a major crustal deformation zone which was dominated by simple shear. The comparison with our modelling suggests a finite shear strain of approximately 5 gamma, which in turn implies a lateral displacement of 400 km parallel the Sefwi Greenstone Belt, which places Southern Ghana (EoGhana?) near eastern Burkina Faso prior to deformation. Our analysis also suggests that the leucogranites were already acting as more rigid bodies during the shearing, suggesting that their emplacement was predominantly pre-kinematic.

1. Introduction

The southern part of the Palaeoproteroic part of the West African Craton consists for the most part of a series of sub-parallel NE-trending greenstone terrains, separated by either tonalite-trondhjemite-granodiorite (TTG) and granite domains or sedimentary basins affected by pervasive folding. The geodynamic evolution of the region remains the subject of considerable debate, and the resolution of key questions is hindered by the relatively limited outcrop. Although a broad stratigraphy has been established within individual greenstone belts, questions which rest include the nature of the relationship between adjacent greenstone belts (is each belt a single basin, or has subsequent deformation restructured the region (Ama Salah et al., 1996; Baratoux et al., 2011; Dampare et al., 2008; Feybesse et al., 2006; Metelka et al., 2011)), the relationship between deformation and granitoid emplacement (does granite emplacement drive deformation (Lompo, 2010; Vidal et al., 2009)), or vice versa (Baratoux et al.,

2011); are specific granitoids synkinematic (Feybesse et al., 2006), and the kinematic significance of localised late shears (do they represent major displacements (Ledru et al., 1991), or simply readjustment of mechanical blocks during bulk shortening (Vidal et al., 2009)).

This study uses field observations combined with the regional geophysical data available for the Sefwi Greenstone Belt and the adjacent Sunyani Basin in South-West Ghana (which is known as the Comoé basin in South-East Ivory Coast, so we will use the combined Sunyani-Comoé Basin to describe this basin) to investigate the geometric, kinematic and dynamic behaviour of a suite of leucogranites which intrude the basin sediments, based on the idea that we can use granites as markers of the large-scale kinematic framework (Debacker and Sintubin, 2008; Feybesse et al., 2006; Roman-Berdiel et al., 1997). The interpretation of their behaviour is in turn based on finite element modelling of idealised two-phase systems, using the Elle modelling platform (Bons et al., 2008; Jessell et al., 2001, 2009). In this study we investigate the mechanical behaviour of a system that at the scale of observation can be considered to be a deformed two-phase system: a series of leucogranite plutons and their host sediments. The mechanical evolution of two-phase systems in rocks has been a subject of detailed

* Corresponding author.
E-mail address: mark.jessell@ird.fr (M.W. Jessell).
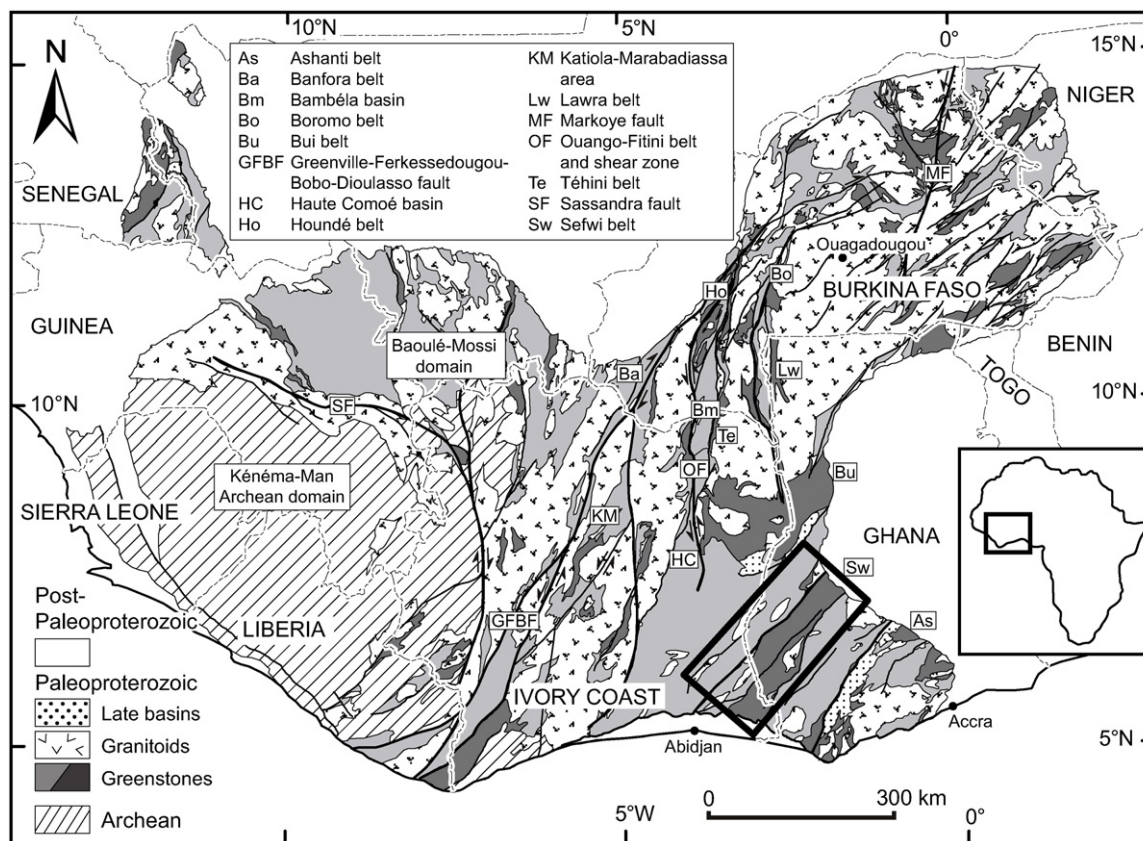
Fig. 1. Simplified geological map of the Leo-Man craton (modified after Milési et al., 2004) with the zone of interest outlined; the Paleoproterozoic greenstones are divided into: light grey – intermediate to acid volcano-clastics and volcano-sediments, dark grey – mafic to intermediate lavas and volcanic products.

field, laboratory and numerical studies for several generations. These studies have in general investigated two principal aspects of the problem: the bulk mechanical behaviour of the system, and the flow field leading to the change in shape and/or rotation (or non-rotation) of the more rigid phase with respect to an external reference frame (see Jessell et al., 2009 for bibliography on this subject). In this paper we focus on the application of previous studies of two-phase systems to the interpretation of last major deformation event seen in the Sefwi-Sunyani-Comoé region.

2. Geological setting

### 2.1. The Baoulé-Mossi Paleoproterozoic domain

The oldest rocks in West Africa are Archean in age (>2500 Ma) and are found in western Ivory Coast, Liberia, Sierra Leone and southern Guinea. They consist of felsic and mafic gneisses and migmatites associated with narrow greenstone belts of lower grade but still metamorphosed supracrustal rocks consisting of tholeiitic basalts and metasediments including turbidites, conglomerates and extensive banded iron formation.

The Baoulé-Mossi domain (Fig. 1) is found to the north and east of the Archaen domain (Bessoles, 1977). The Paleoproterozoic domain is characterised by the typical Archean-like greenstone-granitoid assemblages that principally consist of volcanic, volcano-sedimentary, and sedimentary sequences separated by extensive tonalite-trondhjemite-granodiorite and granite provinces. The volcanic and volcano-sedimentary rocks belong to the Birimian Supergroup, which is thought to have formed in the context of volcanic arcs and oceanic plateaus (Abouchami et al., 1990; Béziat et al., 2000; Boher et al., 1992; Leube et al., 1990;

Pouclet et al., 1996; Taylor et al., 1992). Radiometric dating of the volcanic units (Davis et al., 1994; Lüdtke et al., 1998, 1999) places the main peak of the Birimian volcanism at around 2190–2160 Ma, while detrital zircons from the sedimentary basins yield ages as young as 2130 Ma (Lüdtke et al., 1999) or 2107 Ma (Doumbia et al., 1998). The Birimian volcanic and volcano-sedimentary units are unconformably overlain at several places across the craton by detrital shallow water sedimentary rocks, which are known as the Tarkwaian sediments (Feybesse et al., 2006; Leube et al., 1990; Oberthür et al., 1998; Sestini, 1973; Whitelaw, 1929). The whole complex of volcanic, volcano-sedimentary and sedimentary units has been intruded by several generations of granitoids, which were emplaced during discrete magmatic pulses from 2180 to 1980 Ma (Agyei Duodu et al., 2009; Castaing et al., 2003; Doumbia et al., 1998; Gasquet et al., 2003; Hirdes et al., 1996; Leube et al., 1990; Naba et al., 2004; Pons et al., 1995; Siegfried et al., 2009; Thomas et al., 2009). The general geochemistry of the granitoids evolves from Na-rich calc-alkaline to K-rich alkaline (Boher et al., 1992) while their shape depends on the tectonic regime during their emplacement, ranging from undeformed circular plutons to elongated and complex interlocked bodies (Pons et al., 1992, 1995).

2.2. Tectonic evolution

The Baoulé-Mossi domain developed during the Eburnean orogeny (Bonhomme, 1962), which operated between ~2130 and 1980 Ma (Davis et al., 1994; Feybesse et al., 2006; Oberthür et al., 1998). Most of the volcanic and sedimentary rocks underwent lower to upper greenschist facies metamorphism (Béziat et al., 2000; Feybesse et al., 2006; Ganne et al., 2012; Křibek et al., 2008), and although John et al. (1999) and Galipp et al. (2003) report lower amphibolite facies in Ghana with regional MP/MT conditions
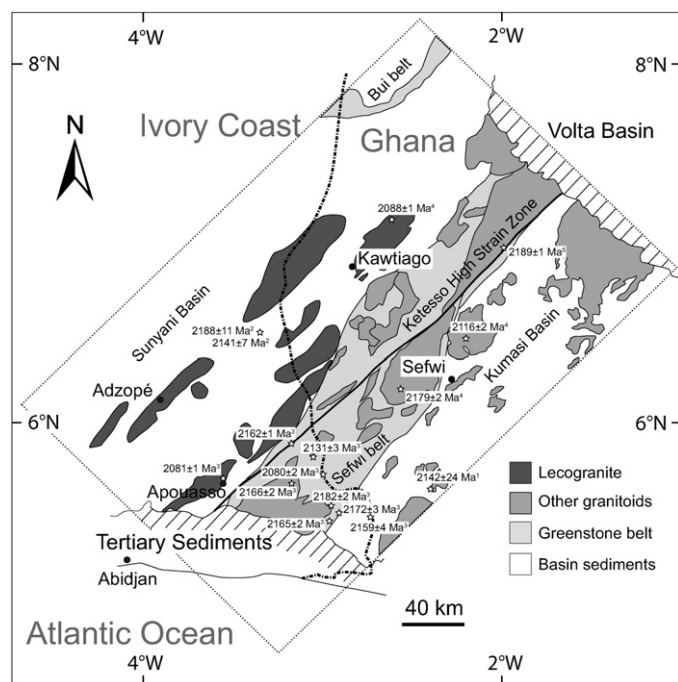
Fig. 2. Simplified map of SW Ghana and SE Ivory Coast (after Ghana 1:1M sheet: Agyei Duodu et al. (2009) and CI 1:200K sheets: Adou et al. (1995), Delor et al. (1992), Simeon et al. (1992), Yao et al. (1995)), showing previously reported ages, taken from the following sources: (1) Adadey et al. (2009), (2) Adou et al. (1995), (3) Delor et al. (1992), (4) Hirdes et al. (1992) and (5) Hirdes and Davis (1998).

reaching (500–600 °C, 5–6 kbar). The Eburnean orogeny is generally divided into two major deformation phases. The first phase, which caused major crustal thickening (Allibone et al., 2002a; Boher et al., 1992; Feybesse et al., 2006; Milési et al., 1992; Vidal et al., 2009), operated approximately during 2130–2100 Ma. The second phase that continued up to 1980 Ma was responsible for the formation of regional scale transcurrent shear zones and faults, which transect all lithologies. Gold mineralisation in West Africa is generally related to these shear zones (Allibone et al., 2002a,b, 2004; Blenkinsop et al., 1994; Bourges et al., 1998; Feybesse et al., 2006; Milési et al., 1989, 1992). The consolidated Eburnean basement was then locally affected by a N–S oriented compressional event (Baratoux et al., 2011; Debat et al., 2003; Hein, 2010; Nikiéma et al., 1993) and unconformably overlain by the Neoproterozoic sediments of the Taoudeni, Iullemeden and Volta basins. Dyke swarms cross the entire Proterozoic domain in several directions and are formed by at least six different generations (Jessell et al., 2010).

2.3. The Sefwi-Sunyani-Comoé region in Ghana and the Ivory Coast

The Birimian terrane of SW Ghana and the Ivory Coast is characterised by a series of parallel NE–SW trending greenstone belts separated by sedimentary basins, and this study focuses on the Sefwi Greenstone Belt and the Sunyani-Comoé Basin in central Ghana and SE Ivory Coast (Fig. 2). The greenstone belts are typically less than 100 km wide but can be up to 800 km long. The Sefwi Greenstone Belt predominantly consists of metamorphosed tholeiitic lavas, some volcaniclastics, minor sediments as well as synvolcanic tonalitic to granodioritic granitoids (see maps of Adou et al., 1995; Agyei Duodu et al., 2009; Delor et al., 1992; Hirdes et al., 2007). Hirdes and Davis (1998) have obtained a U–Pb zircon age for a rhyolite from this belt at 2189 ± 1 Ma, while U–Pb zircon ages for granitoids within the belt lie between 2180 and 2170 Ma (Hirdes et al., 1992).

The Sunyani-Comoé sedimentary basin contains dacitic volcaniclastics, wackes, argillites and at their margins chemical sediments (Leube et al., 1990). The Birimian sedimentary basins are derived mainly from the adjacent greenstone belts (Davis et al., 1994) and extensive Birimian sedimentation took place simultaneously with Birimian belt volcanism but probably outlasted Birimian volcanic belt formation in Ghana.

The Sunyani-Comoé basin is intruded by numerous granitoids varying in composition from tonalite to peraluminous granite. Zircons in the leucogranites immediately adjacent to the Sefwi Belt give ages of 2088 ± 1 Ma (Hirdes et al., 1992, for the Kawtiago Granite, Ghana) and 2081 ± 1 Ma (Hirdes et al., 2007 for the Apouasso Granite in the Ivory Coast) which provide a lower limit to the age of sedimentation. Regional scale mapping (Agyei Duodu et al., 2009) shows that they are typically but not exclusively elongate in a NE direction, and published field studies show internal deformation microstructures with a sub-vertical foliation and sub-horizontal stretching lineation, both of which are parallel to their elongation direction (Vidal et al., 2009). They are peraluminous and consist of albite-rich plagioclase, microcline, quartz with relatively little mica and biotite.

In this region, two opposing models have been proposed for the emplacement of the late leucogranites into the Sunyani-Comoé Basin. Based on the proximity and geometry of the elongate leucogranites with respect to the mapped shear zones Feybesse et al. (2006) proposes that the leucogranites were synkinematically emplaced during major transcurrent shearing nucleated from earlier brittle fractures (Fig. 3a). In contrast, based on the vertical internal foliations within the leucogranites and the plutons' relationship with fold and shear structures found in the basin sediments, Vidal et al. (2009) envisage early diapiric emplacement of the plutons with subsequent horizontal compression followed by minor shearing localised around pluton margins (Fig. 3b). Their evidence for a diapiric emplacement of the plutons is based on their interpretation of normal-type, down-dip movements along the pluton boundaries, within the leucogranites and surrounding rocks and apparent increases in pressure estimations around the plutons.

Structural and petrological constraints for this study are provided by field studies in the Kawtiago region of Ghana (Amponsah, 2012), and the three principal rock types found in the area are described below. The field study concentrated on the deformation within the Sunyani-Comoé basin, as we are interested in the youngest deformation events, and these sediments postdate the earlier Eburnian deformation events. In the basin, two structural events can be seen, the emplacement of the leucogranites, and the deformation of the sediments (with both folding and localisation into shear zones).

2.3.1. Greywacke

Fresh samples of fine- to medium-grained greywacke were observed in four unoriented drill cores from boreholes drilled by Keegan resources west of Kawtiago. The greywacke shows sub-vertical to vertical penetrative foliation. Some of the greywacke outcrops show mineral lineations, mainly trending 040° and plunging 20° towards the NE. In thin section (Fig. 4a), the metagreywacke has a fine to medium grained texture and is composed mainly of gently deformed quartz, chlorite and micas with plagioclase feldspar, sphene, pyrites and tourmaline as accessory minerals.

2.3.2. Phyllites

The phyllites were very difficult to observe in the field due to the extent of weathering in the area; however fresh samples were obtained in five drill cores samples. The phyllites within the drill cores which were in contact with the leucogranites were slightly harder, which may be the result of contact metamorphism associated with the emplacement of the granite. The phyllites also show a

a)

Granitoids

Basin sediments

Greenstone belts

~10 km

b)

i)

~25 km

ii)

~25 km
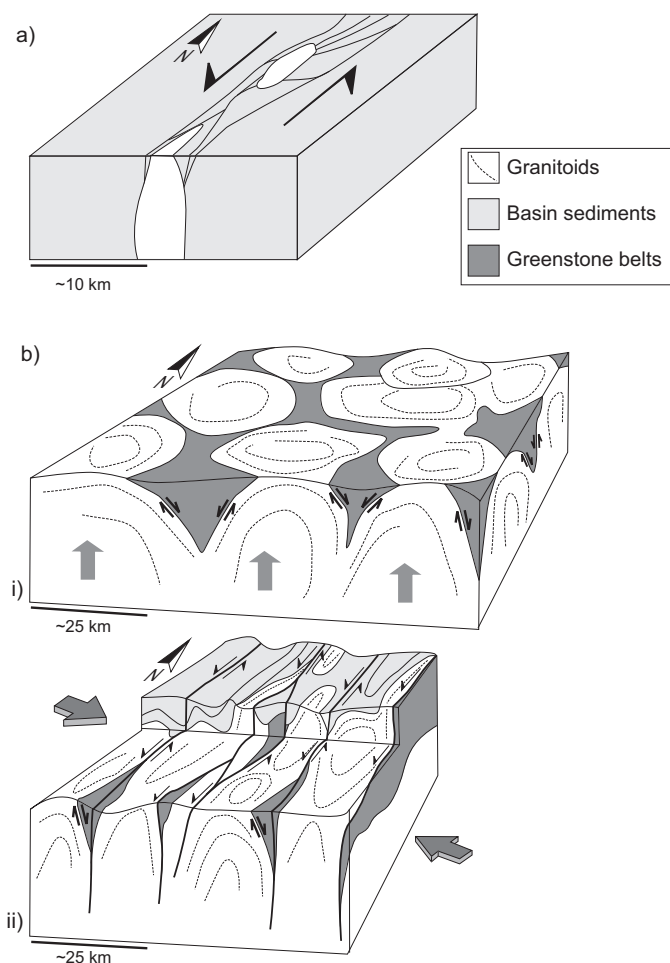
Fig. 3. Current models for Sunyani-Comoé Basin leucogranite emplacement and subsequent deformation. (a) Model of Feybesse et al., which consists of the synkinematic emplacement of leucogranites in ductile shears which nucleated from brittle precursors. (b) Model of Vidal et al., which consists of (i) an early phase of gravity-driven granitic doming with concurrent gravitational collapse of the greenstone belts followed by (ii) subsequent compression and late shearing.

subvertical to vertical penetrative foliation. The phyllites are commonly intercalated with the metagreywackes in the drill core.

In thin section, it is composed mostly of quartz, micas, pyrite and graphite and shows a marked crenulation cleavage (Fig. 4b). The larger grains of quartz are anhedral and show sweeping undulose extinction, whereas the smaller quartz grains do not exhibit any undulose extinction, but have serrated edges.

2.3.3. Leucogranites

The leucogranites are slightly weathered in outcrop and are whitish grey and phaneritic. They have quartz and pegmatite veins intruding through them. The rock is coarse-grained and variably deformed, with a granular texture, composed of quartz, plagioclase, microcline, muscovite, biotite and accessory minerals such as sphene and zircons. The quartz grains show extensive tabular sub-grains, and the grain boundaries are irregular suggesting significant grain boundary migration (Fig. 4c and d). Together these observations suggest medium to high temperature (but solid-state) deformation (Passchier and Trouw, 2005).

3. Regional geophysical data

The regional airborne magnetic data for this study made use of three surveys in Ghana and the Ivory Coast which have been combined into a single stitch (Fig. 5a), here represented as a Total Magnetic Intensity image (colour information) draped over a first vertical derivate of the Total Field (brightness information). The gravity data (not shown here) is exclusively ground based, and is much more widely spaced. Radiometric (Gamma Ray spectroscopic) and Landsat satellite data were available for the Ghana area, but were not found to be particularly useful given the dense forestation. The magnetic images cover the 500 km strike length of the Sefwi-Sunyani-Comoé region, which is overlain to the NE by the Neoproterozoic sediments of the Volta Basin in Ghana and to the SW by Paleogene-Neogene age sediments and then the Atlantic Ocean in the Ivory Coast. A number of the lithologies described by previous workers in this region show characteristic magnetic signatures that help to better define their map extent (Fig. 5b), which is often masked by the significant thicknesses of lateritic alteration.

Detailed mapping of foliation–pluton interactions is extremely challenging due to the poor outcrop conditions in the region, however if we zoom in on the small pluton east of Adzopé (Fig. 5c and d), we can see in both the magnetic data and the map of Adou et al. (1995) that the foliation and metamorphic aureole form tails parallel to the long axis of the larger Adzopé pluton.

The leucogranites show up as gravity lows and as round to elongate zones of homogenous low magnetic intensity in this region (the high frequency NW striping in the Ivory Coast data is an artefact of the geophysical processing).

The sediments either side of the Sefwi Belt (the Sunyani-Comoé Basin to the North-West, and Kumasi-Afema basin to the South-East) are variably magnetic, cut by linear structures, which are clearly dykes with various orientations, the most obvious of which trend N–S. There is a spatial correlation between more magnetic sediments and the leucogranites, although their geometry does not suggest simple metamorphic haloes. These strongly magnetic sediments often envelope the leucogranites, and also form NW–SE oriented "tails". Field work in the Kawtiago region in Ghana shows that these more magnetic sediments are greywackes, with the less magnetic sediments being predominantly phyllites.

The South-East region of the Sefwi belt proper is transected by a strong linear magnetic high (which corresponds in Ivory Coast to the Ketesso High Strain Zone of Hirdes et al., 2007), which in the regional magnetic data can be seen to continue another 250 km beneath the Volta Basin. It is cut by the N–S dykes (as yet undated). The volcanics, volcano-sediments and early granitoids of the Sefwi Greenstone Belt appear to be cut by and entrained in the deformation caused by the Ketesso High Strain Zone. In the field, this feature shows a sub-horizontal stretching lineation (Hirdes et al., 2007).

4. Kinematic analysis of the leucogranites and their host sediments

The elongate rounded forms of the leucogranites, together with their enveloping sediments suggest that we may be able to use their geometries to unravel the regional kinematics. To do this we draw upon and extend the work of Jessell et al. (2009) who undertook a systematic analysis of the predicted geometries of two-phase materials with two distinct viscosities. Jessell et al. (2009) only considered bulk simple shear; however, since the deformation geometry at the time of the deformation of the leucogranites has not been conclusively determined, we extend the analysis here to pure shear deformation.

4.1. Deformation partitioning in two-phase systems

The experiments of Jessell et al. (2009) use the Elle and Basil (Houseman et al., 2008) modelling codes to systematically vary the viscosity ratio, the percentage of "hard" phase and the stress
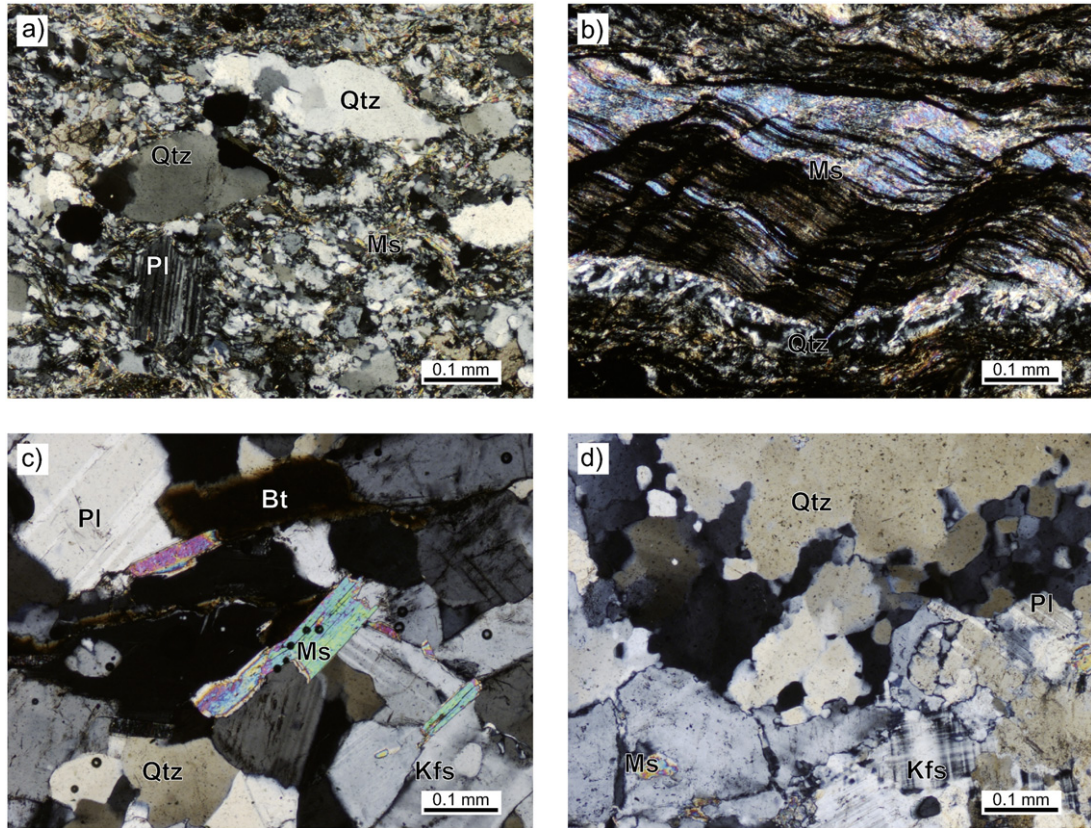
Fig. 4. Microphotographs of the major rock types from the Kawtiago region, Ghana. Cross-polarized light. (a) Greywackes showing weak to moderate strain, (b) crenulated phyllites, (c) weakly deformed leucogranite and (d) deformed leucogranite showing high temperature grain boundary migration and sub-grain microstructures. (For interpretation of the references to color in this figure legend, the reader is referred to the web version of the article.)
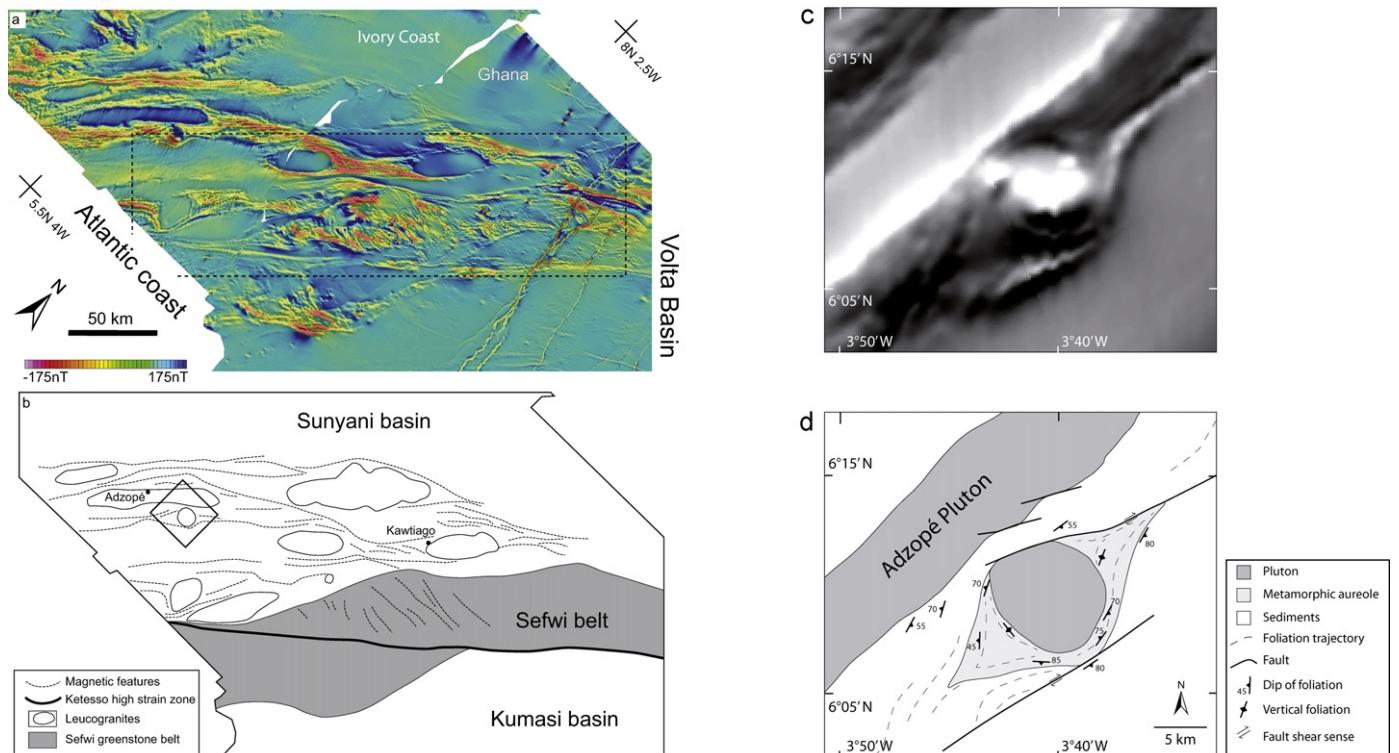
Fig. 5. (a) Airborne magnetic image of the Sefwi Belt. Colours reflect residual magnetic intensity, brightness reflects the first vertical derivative of the magnetic field, dashed rectangle shows region covered by Fig. 12. (b) Sketch showing principal features of interest seen in magnetic data, with solid oblique rectangle showing region covered by parts (c) and (d) of this figure. (c) Zoom of magnetic data for region east of Adzopé, showing magnetic units wrapping around small pluton. (d) Map of region east of Adzopé, showing foliation trajectories in sediments and metamorphic aureole associated with small pluton (after Adou et al., 1995).

Table 1
Experimental conditions of numerical simulations for two-phase systems.

Experiment number	Deformation geometry	% Hard phase	Viscosity ratio	Stress exponent	Effective viscosity ratio	Finite strain
5_30_1	Simple shear	30	5	1	5	7.5γ
5_50_1	Simple shear	50	5	1	5	7.5γ
5_70_1	Simple shear	70	5	1	5	7.5γ
10_30_1	Simple shear	30	10	1	10	7.5γ
10_50_1	Simple shear	50	10	1	10	7.5γ
10_70_1	Simple shear	70	10	1	10	7.5γ
5_30_3	Simple shear	30	5	3	15	7.5γ
5_50_3	Simple shear	50	5	3	15	7.5γ
5_70_3	Simple shear	70	5	3	15	4γ
10_30_3	Simple shear	30	10	3	46	4γ
10_50_3	Simple shear	50	10	3	46	4γ
10_70_3	Simple shear	70	10	3	46	3γ
ps5_30_1	Pure shear	30	5	1	5	85%

exponent to provide a wide range of models of two-phase deformation to relatively high strains (up to 7.5γ, Table 1). In these experiments we were able to demonstrate that in terms of the final geometry and strain patterns, for the case of more rigid objects in a softer matrix, it did not matter if we modelled linear viscous materials (stress exponent = 1) of high viscosity contrast or non-linear materials (stress exponent > 1) with a lower viscosity contrast (see Jessell et al., 2009 for more details). As a consequence for the current analysis we will use the Effective Viscosity Ration (EVR) whilst recognising that the stress-exponent cannot be constrained by analysis of the final geometries. These two-dimensional numerical experiments were originally carried out to study grain scale phenomena, and thus show grain boundaries, however the viscous deformation code is non-dimensional and the grain boundaries here simply act as passive markers. Fig. 6a shows the outcomes of these calculations for those models which had 30% (grey, which is more viscous for effective viscosity ratios less than 1, and less viscous for those greater than 1) of one phase and 70% (white) of the second phase, sorted from top to bottom of the figure in terms of effective viscosity ratio. In this figure we can see systematic variations with respect to both effective viscosity ratio (EVR) and finite strain, so that we can imagine using these models as a "template" to simultaneously estimate both shear strain and effective viscosity ratio, if of course we can be sure that the region underwent bulk simple shear. Visual inspection of this template suggests that the leucogranites were acting as more rigid objects in a softer matrix, and we will examine the evidence for and implications of this hypothesis in more detail in the subsequent sections. In this paper we include information from an additional pure shear model (Fig. 6b) (30% hard phase, EVR = 10, 85% shortening) to see if we can distinguish between pure and simple shear deformation in the Sefwi-Sunyani-Comoé region.

Apart from the ability to predict the evolution of the shapes of the hard and weak phases during deformation, by superimposing a regular square grid on the starting materials we can readily visualise the strain variations as the experiments progress. In Fig. 7, we show one such deformed grid for a viscosity ratio of 10 and a linear stress exponent at a dextral shear strain of 5γ. The original grid consisted of sets of horizontal lines (red), and vertical lines (dark grey). We can see that there are marked zones of localisation of deformation which envelope the more rigid objects, but extend long distances into the matrix material. As a result, the matrix is partitioned into distinct elongate zones of dominant pure and simple shear which both stair-step up the model from lower-left to top right. The higher viscosity objects themselves, on the other hand, as predicted by Eshelby's (1957) analysis of equivalent elastic two-phase systems, show very homogeneous deformation grids, with only gentle variation in orientation and intensity across the zone. This correlates well with the observation in the magnetic image of uniform magnetic intensities.

4.2. Circularity vs elongation axis

By analogy with similar studies on smaller scale structures (Dunnet, 1969; Lisle, 1977; Ramsay, 1967), we can compare the deviation from circularity of the more rigid bodies (in this case the leucogranites) with the orientation of their long axes. In this study, since the granites show very smooth contacts at the regional scale, and are often deformed in non-elliptical geometries, in place of the more traditional elliptical axial ratio, we use the circularity index (Lira and Pina, 2009; Zunic and Hirota, 2008) C:

$$C = 4\pi \left(\frac{A}{l}\right)^2$$

where A is the area and l is the perimeter length, and compare it with the orientation of the long axis of the object (this time using a best fit ellipse to define the direction). Fig. 8a shows the starting material (dark regions are more viscous) and the relationship between circularity and long-axis orientation in the more viscous material prior to deformation, and we can see a broad spectrum of orientations, with a slight preponderance of orientations near 0°. If we deform this starting material in simple shear to a strain of (7.5γ) we can see a general trend towards more circular regions at higher angles (Fig. 8b). There is a general decrease in circularity, however some regions retain a shape close to their initial circularity. In contrast if we deform the same starting material in pure shear to a shortening of 84% (Fig. 8c) we can see that the orientation distribution has collapsed down to a range less than 10° from 0°, and the overall circularity of the more viscous regions has also decreased. Finally if we plot the Sunyani-Comoé leucogranites, we can see a wide range of long axis orientations, with a trend towards more circular geometries at higher angles (Fig. 8d). For this analysis we have used the Ketesso High Strain Zone (Fig. 3) as the reference for the 0° direction as this is a 500-long km structure that in the regional magnetic data shows a clear involvement in leucogranite deformation (especially in the SE of the study area).

4.3. Circularity vs area

In the simple shear experiments, we noticed a tendency for smaller regions to retain their circular form, even to high strain, so to test this we also plotted circularity against area. Fig. 9a shows the starting material, which displays a slight tendency towards less circular forms for regions with larger areas. The simple shear experiment shows a marked evolution with a strong inverse relationship between circularity and area (Fig. 9b). If we plot the pure shear experiment (Fig. 9c) we can see that the circularity-area relationship has effectively been translated parallel to the circularity axis, but has otherwise not evolved significantly. Again the plot of
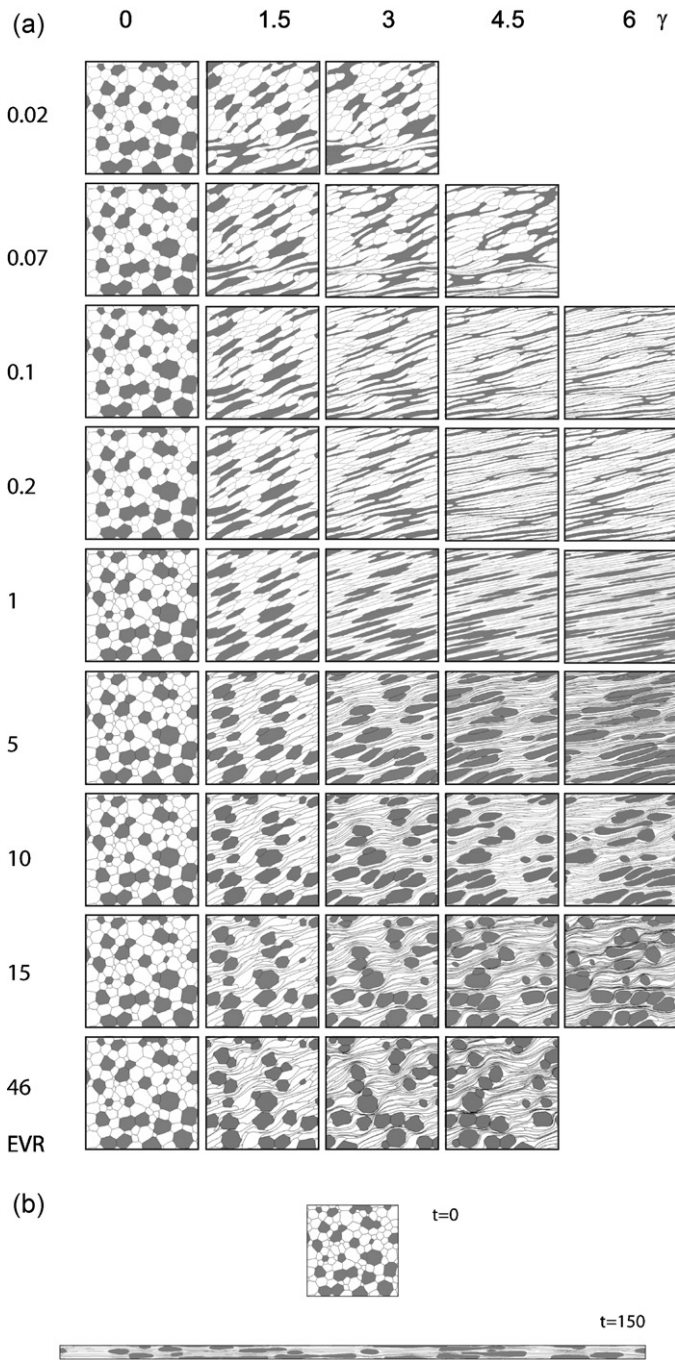
Fig. 6. Mechanical modelling of two-phase systems in pure and simple shear. The grey phase is 30% of the area of the model, the white phase 70%. (a) Simple shear experiments. For each row the progressive deformation of a two-phase system with the stated effective viscosity ratio (EVR) is shown. The effective viscosity ratio between the grey and the white phases increases systematically down the figure. Not all experiments could be carried out to high strain as severe localisation of deformation occurred for some conditions. All experiments had cyclic horizontal and vertical boundaries. (b) Pure shear experiment before and after deformation, for a model with 30% hard phase, an EVR of 10 and 85% shortening.

Sunyani-Comoé leucogranites apparently follows the trend shown by the simple shear experiment (Fig. 9d).

4.4. Paleorheology and strain estimates

If we accept that the circularity-orientation and circularity-area analyses provide good evidence for a strong simple shear
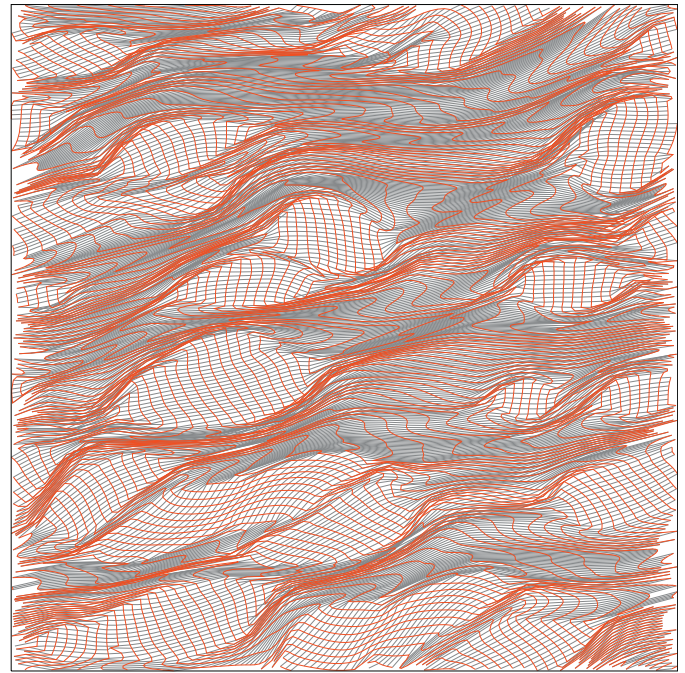
Fig. 7. Now-deformed but originally square grids reveal deformation localisation as well as partitioning into different deformation geometries. Red lines (dark grey in black and white) were originally horizontal, grey lines vertical (light grey in black and white). For this particular image the viscosity ratio was 10 between more and less viscous phases, the stress exponent was 1, and the shear strain was 5γ. A strong partitioning between the hard and soft phases is evident, both in terms of finite strain and strain geometry, with the harder phase deforming predominantly by pure shear, and the weaker phase deforming in a more complex fashion, itself showing strong partitioning. (For interpretation of the references to color in this figure legend, the reader is referred to the web version of the article.)

component to the deformation, then we can go a step further and try to simultaneously estimate the finite shear strain and the viscosity ratio of the leucogranites and their hosts. If we only had the shapes of the leucogranites, this simultaneous inversion would not be possible, as there is a trade-off between the elongation of an elliptical object during progressive deformation and the relative viscosity of the objects and the matrix: an ellipse of a given form can either be the result of low strain and a low viscosity contrast or a higher strain and a proportionally higher viscosity contrast. This dilemma can however be resolved in the case of the sediments of the Sunyani-Comoé basin, as the patterns of NE–SW trending stratigraphically-controlled magnetic highs (Fig. 5) correlate well with the patterns of localisation of deformation seen in the mechanical models, and as with the model the region is divided up into elongate zones. We can thus use the combination of localisation patterns in the sediments with the form of the leucogranites to estimate (obviously only to a first-order) that the finite shear strain was around 5γ and the effective viscosity ratio between leucogranites and the host sediments was around 7:1.

5. Discussion

5.1. Caveats

(a) Our ability to compare our mechanical modelling with the natural laboratory of the Sefwi region is in part helped by the fact that the deformation of the leucogranites is the last significant deformation event to occur in this region. Nevertheless we recognise that for this analysis to work, we have to demonstrate that the deformation was effectively 2D plane strain parallel to
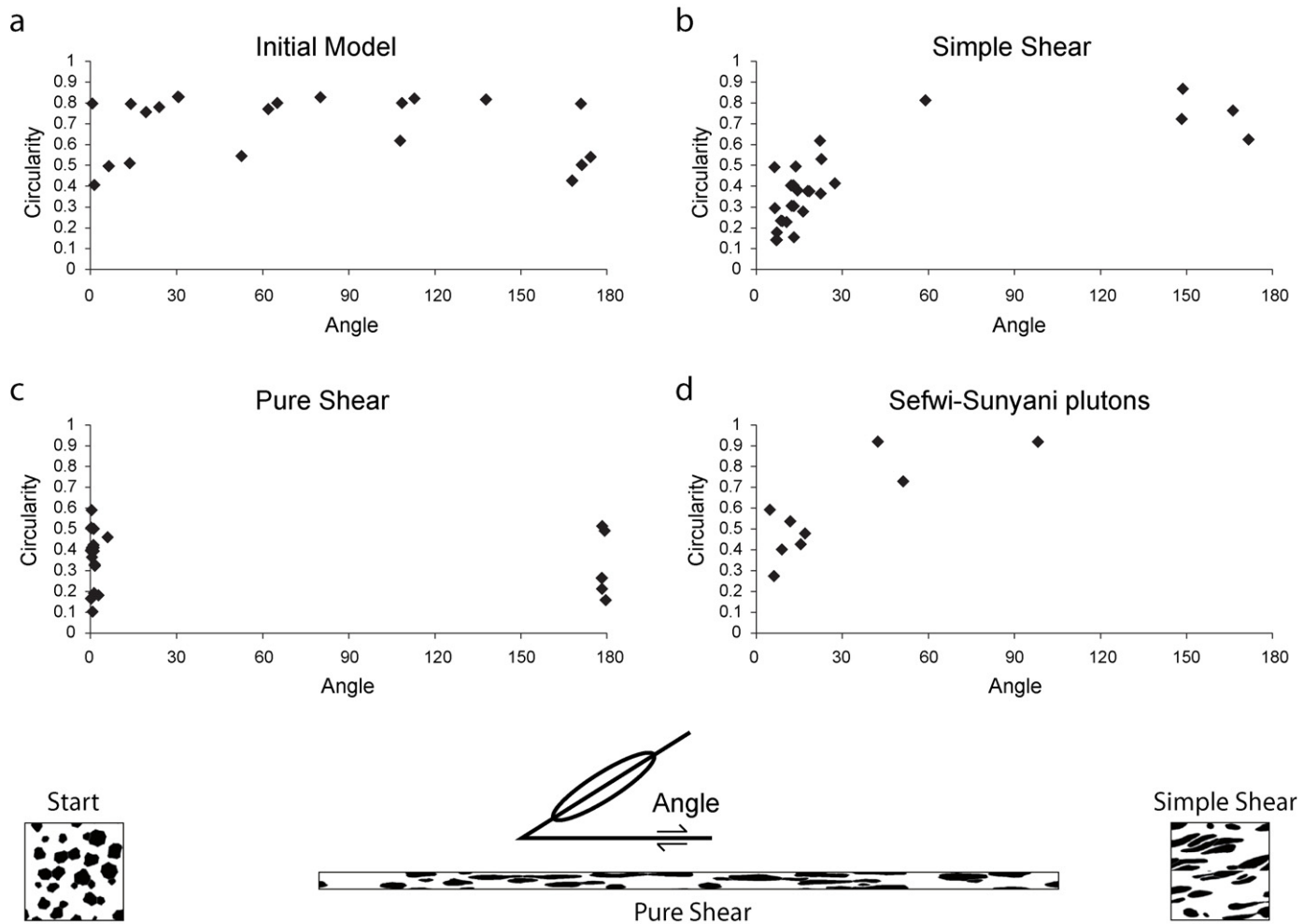
Fig. 8. Plots of circularity versus orientation of the long axis of the more rigid objects. (a) Starting relationship for the input model for the numerical experiments, which shows a generally uniform distribution of circularity with respect to orientations. (b) Final relationship for the simple shear experiments, which shows a decrease in circularity as the long axis of the object approaches the flow plane. (c) Final relationship for the pure shear experiments, which shows a decrease in circularity for all objects coupled with a tight clustering of orientations around normal to the compression direction, regardless of circularity. (d) The relationship seen for the leucogranites, which shows a decrease in circularity as the long axis of the object approaches the flow plane, suggesting a simple shear deformation mode. The sketch below the graphs shows the definition of the angle, and the small insets show the shapes of objects before (left) and after deformation in pure (centre) and simple shear (right).

the Earth's surface. We have two lines of evidence to support this requirement. First the observations of Vidal et al. (2009) that the interior of the leucogranites show a horizontal stretching lineation, and that the Ketesso High Strain Zone also show sub-horizontal stretching lineations (Hirdes et al., 2007) which are consistent with surface parallel plane strain. The second line of argument is that the contacts of the leucogranites themselves are steeply dipping. This is based on field observations by Hirdes et al. (2007), and on 2D gravity modelling (not shown here), which both suggest pluton margin dips of 70–80°. The Ketesso High Strain Zone shows foliation dips of between 75° and 88° (Hirdes et al., 2007).

(b) The choice of viscous rheologies for both phases is certainly a simplification, and as we discussed earlier, we do not make a specific assumption of Newtonian (linear) viscous behaviour, as the numerical simulations give the same results for high-viscosity contrast Newtonian and low-viscosity contrast non-Newtonian flow. Nevertheless one of the rare paleo-rheological studies of mid-crustal sediments does suggest a Newtonian viscous response (Kenis et al., 2005).

(c) Unfortunately we do not know starting shape of plutons, however their homogeneous magnetic character suggests that they are formed as single pulses.

(d) Finally we are restricted in our analyses by the number of leucogranites available, for which the Atlantic Ocean and the Volta Basin are to blame, and for which we are unable to see how to improve the statistics other than by performing high resolution geophysical surveys over the Volta Basin.

5.2. Paleorheology

Although the rheologies of common crustal rocks such as granites are relatively well determined (Dell'Angelo and Tullis, 1988; Tullis and Yund, 1977), sediments are more poorly constrained as the number of deformation processes that are simultaneously active in polymineralic rocks make scaling of laboratory flow laws to natural conditions particularly difficult. In addition, at the scale we are working on, the sediments deform by folding, whereas the leucogranites deform more homogeneously, so that their relative rheologies are very difficult to predict. The mechanical analysis we present here suggests that the Sunyani-Comoé leucogranites were deformed after their emplacement and cooling, since they are acting as more viscous objects relative to the basin sediments, with a relative viscosity of around 7:1. Although these sediments locally achieve amphibolite grade near the leucogranites themselves, on
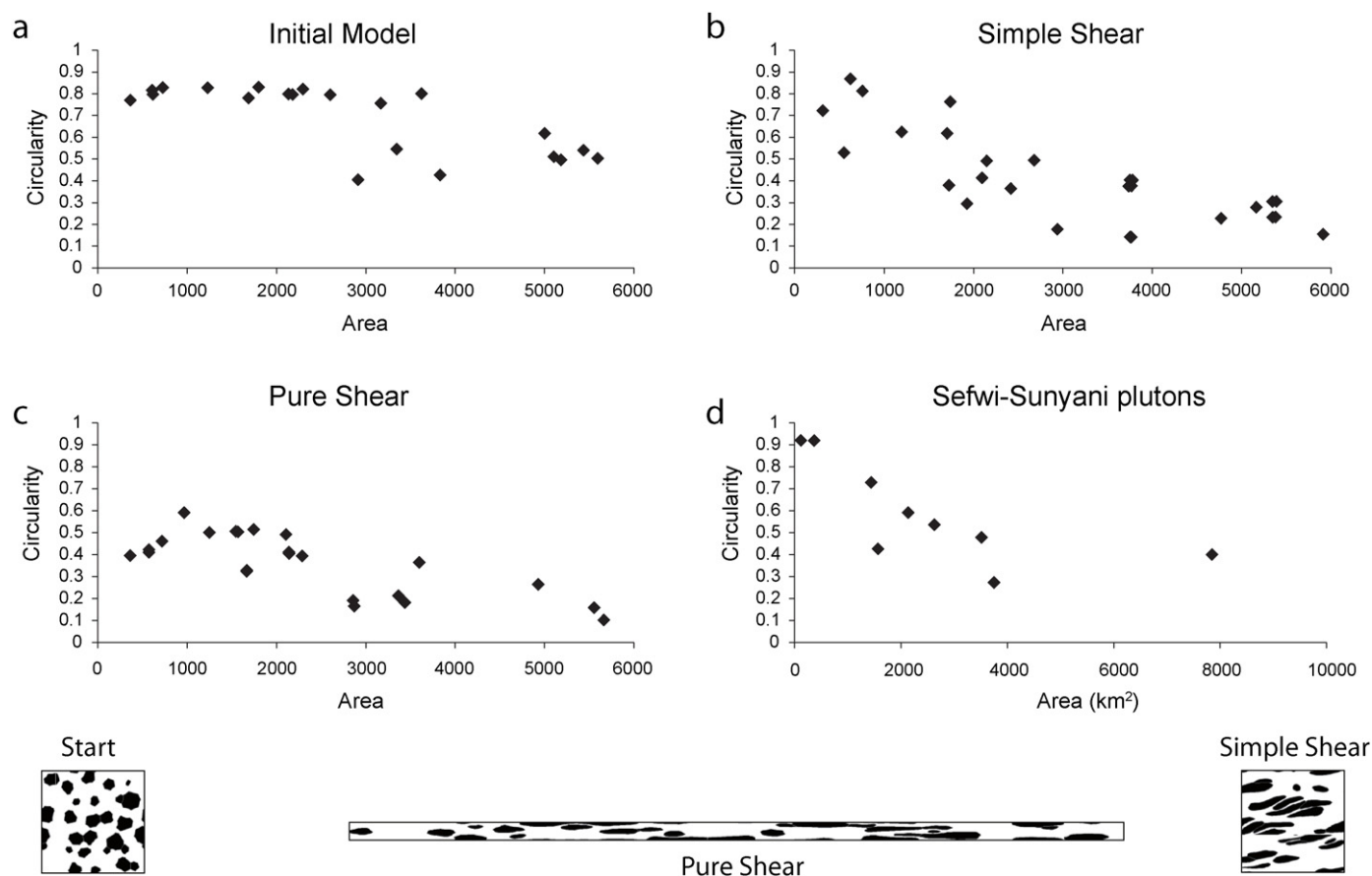
Fig. 9. Plots of circularity versus area of the more rigid objects. (a) Starting relationship for the input model for the numerical experiments, which shows a slight decline in circularity for larger objects. (b) Final relationship for the simple shear experiments, which shows a strong decline in circularity for larger objects. (c) Final relationship for the pure shear experiments, which shows a decrease in circularity for all objects independent of shape. (d) The relationship seen for the leucogranites, which shows a strong decrease in circularity for larger objects, suggesting a simple shear deformation mode. The small insets below the graphs show the shapes of objects before (left) and after deformation in pure (centre) and simple shear (right).

a regional scale they are dominated by upper-greenschist facies to lower amphibolite metamorphic minerals (Galipp et al., 2003), and so we can assume that the sediments would have a higher viscosity than a cooling leucogranite body until there is a very low or non-existent melt fraction.

The experimental and theoretical work on the rheology of partial melts, summarised recently by Rosenberg and Handy (2005) suggests that with as low as 7% melt, the mechanical properties of a partially molten rock will drop by up to two orders of magnitude. Given that our rheological template suggest that the leucogranites are half an order of magnitude stronger than the sediments they intrude, the suggestion by Feybesse et al. (2006) that these bodies were emplaced in a synkinematic shear setting thus seems unlikely. Fig. 5 shows that when there is a dominance of the rigid phase, as one would expect in the case of isolated partially molten plutons in the middle crust, deformation leads to intense localisation by the linking of the low viscosity zones, resulting in extreme smearing into what quickly become fault zones. This type of geometry can been seen in one of the classic synkinematic pluton localities, the South Armorican Shear Zone, in NW France (Berthé et al., 1979; Gapais, 1989; Gumiaux et al., 2004; Truffert et al., 2001), where the southern branch of the shear zone is marked by a 5 m zone of Hercynian highly deformed syn-kinematic leucogranites (Fig. 10a). If we compare the pluton shapes from this area with our mechanical model results for an Effective Viscosity Ratio of 46 in simple shear we can see an excellent correspondence in the geometry of the objects (Fig. 10b). This raises the interesting question as to whether the South Armorican granites were emplaced along a

pre-existing shear zone or whether instead the shear zone was actually nucleated by linking up of deforming plutons. In any case the Sefwi leucogranites do not appear to fall into the class of synkinematic plutons, and did not maintain a low enough viscosity to deform more easily than their host rock after their emplacement.

It is worthwhile considering the likelihood of plutons recording significant deformation during crystallisation, as their capacity to register synkinematic strain is principally a function their cooling rate, the regional strain rate, and the time window over which a plutons crystallises to a mechanical solid state. If we consider the calculated melt fraction for different granitoids as a function of temperature (Fig. 11a, after Bouchez et al., 1992) we can see that leucogranites will contain significant portions of partial melt (well over the 7% rheological threshold) down to just over 640 °C. If we compare this result with the cooling curves for a mid-crustal pluton from (Fig. 11b, after Glazner et al., 2004) we can see that the centre of a 5 km thick, 20 km radius body at 17.5 km depth (not unlike the medium sized plutons we have studied), will take well over million years to attain the solid state (for a geothermal gradient of 20 °C km^{-1}), and the sides, which are what we believe we are seeing at the surface of the Earth today, would take 500,000 years (or approximately 1.6×10^{13} s) to reach the solid state, and larger bodies such as the Adzopé Pluton would take proportionally longer. This of course assumes that the body is emplaced over a short period of time, something we argue for because of the homogeneous internal magnetic signature of the bodies. If we consider probable strain rates between 10^{-14} s^{-1} and 10^{-13} s^{-1} we would expect to see accumulated strains within the leucogranites near

a)

b)
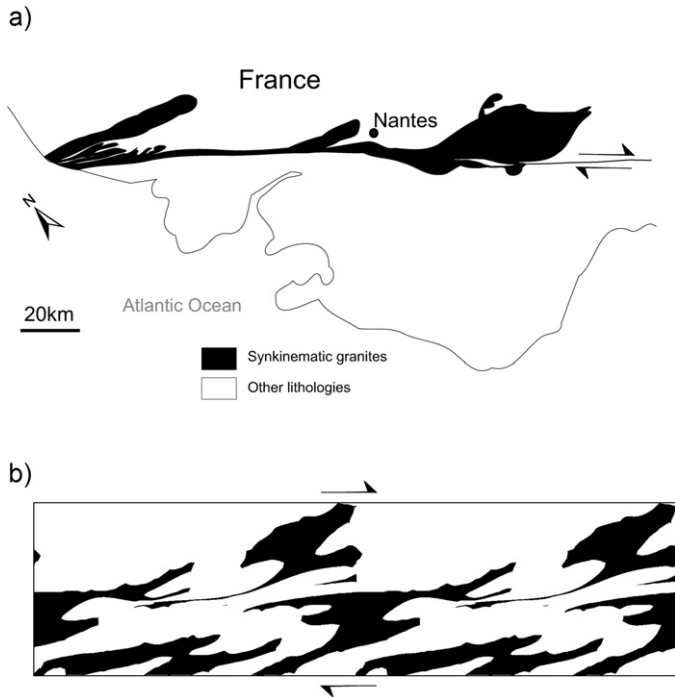
Fig. 10. Sykinematic granites. (a) A map of the granites from the South Armorican Shear Zone, NW France, which are widely accepted to be synkinematic in origin (Roman-Berdiel et al., 1997). (b) A part of the mechanical model (viscosity ratio = 10, stress exponent = 3) with black regions having an effective viscosity 46 times less than the host rock (at γ = 3), which results in extreme localisation of deformation within the less-viscous material and the linking up of initially isolated less-viscous objects. The model is repeated in the horizontal direction to show complete shapes.

the margins of between 0.16 and 1.6γ. The lower level of strain would be difficult to observe, especially if overprinted by a solid-state deformation, and thus the strain state within the pluton is not necessarily a useful indicator of the relative timing of emplacement and deformation.

At the current time we do not have any absolute constraints on the age of the transcurrent shearing, so it may be that the leucogranites were emplaced in a region lacking a sufficiently high ambient strain rate to affect their mode of emplacement, and the notion of "syn-kinematic" emplacement may need to be more precisely defined. If the strain rate relative to cooling age is so low that it will not leave a clear record, perhaps we should call such intrusions "syn-tectonic", i.e. they formed during a period of tectonic activity (which was simply not associated with local deformation at that particular time and place), and leave the term syn-kinematic for those intrusions that show clear evidence of deformation during crystallisation. This distinction is more than just semantic, as it is generally possible to date the crystallisation ages of granitoid rocks; however, the significance of this age increases enormously if we can demonstrate that the pluton was significantly deformed during its crystallisation, as it provides an absolute age for a deformation event. If, however the pluton is merely associated with a period of orogenesis, it can only provide a lower or upper age bracket to deformation events that occur before or after it.

5.3. Kinematics

The predominant simple shear demonstrated by our analyses suggests a more conventional emplacement model followed by transcurrent shearing, which conflicts with the model of Vidal et al. (2009), who suggest a diapiric ascent from a single deep source, followed by compression and then shearing.
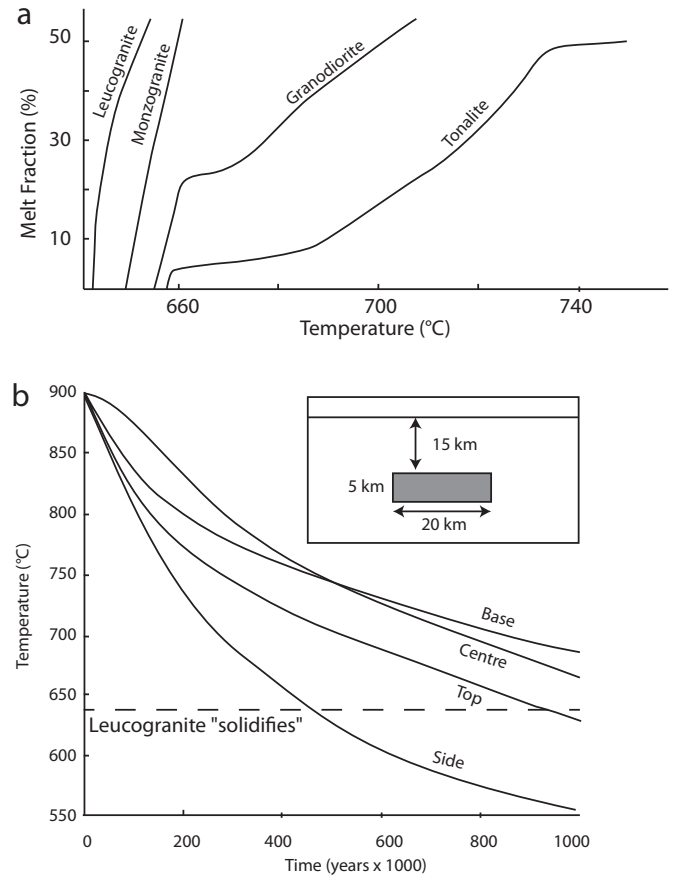
Fig. 11. Constraints on the mechanical behaviour of cooling plutons in a syn-kinematic setting. (a) Melt fraction of silicic magma as function of temperature calculated by using FUSION program of Niederkorn and Blumenfeld (1989). The short cooling times for leucogranites would suggest they are the least likely to be the subject of a synkinematic emplacement for a given strain rate and cooling rate, after Bouchez et al. (1992). (b) Evolution of temperatures in a two-dimensional magma body. The magma body is 5 km thick and 20 km wide, and is emplaced at 15 km depth in an area with a 20 °C km^{-1} geothermal gradient. Inset shows vertical section through the body. The curves show the evolution of temperatures at four points in the body: 1 km below the top centre, in the centre, 1 km above the bottom centre, and 1 km inside the side contact, vertically centred. The horizontal dashed line shows the approximate position of the rheological threshold for leucogranites, suggesting a time to the attainment of significant mechanical strength (<7% melt) relative to the country rock of between 500,000 years to over a million years, depending on the position within the pluton, after Glazner et al. (2004).

If we look at the overall deformation patterns in the Sunyani-Comoé region, including the circularity-orientation analysis shown in Fig. 8, we arrive at a global dextral shear sense, which agrees with some authors intepretations (e.g. Delor et al., 1992), but is contrary to the reported small-scale microstructural evidence for sinistral shearing (Vidal et al., 2009). This conflict can best be resolved in one of two ways. First we can compare this area's evolution with structural histories from adjacent belts such as the Ashanti belt to the South-East. Here an early dominant dextral shear history is overprinted by a minor late sinistral shear sense that is, because it is the final phase of deformation, the one that is best preserved in the microstructures (Allibone et al., 2002b). If we look to the North, in Burkina Faso, there is a strong regional dextral simple shear event that overprints the earlier compressive formation of the greenstone belts (Baratoux et al., 2011). A second factor may also play a role. When one analyses the flow in two-phase systems, one sees that instead of a bulk shear sense dominating across a region, there is a strong partitioning into pure and simple shear domains, and that around the more rigid bodies, there is also a partitioning into zones of synthetic and antithetic shear sense (Bell, 1981; Passchier and

a

50 km

b
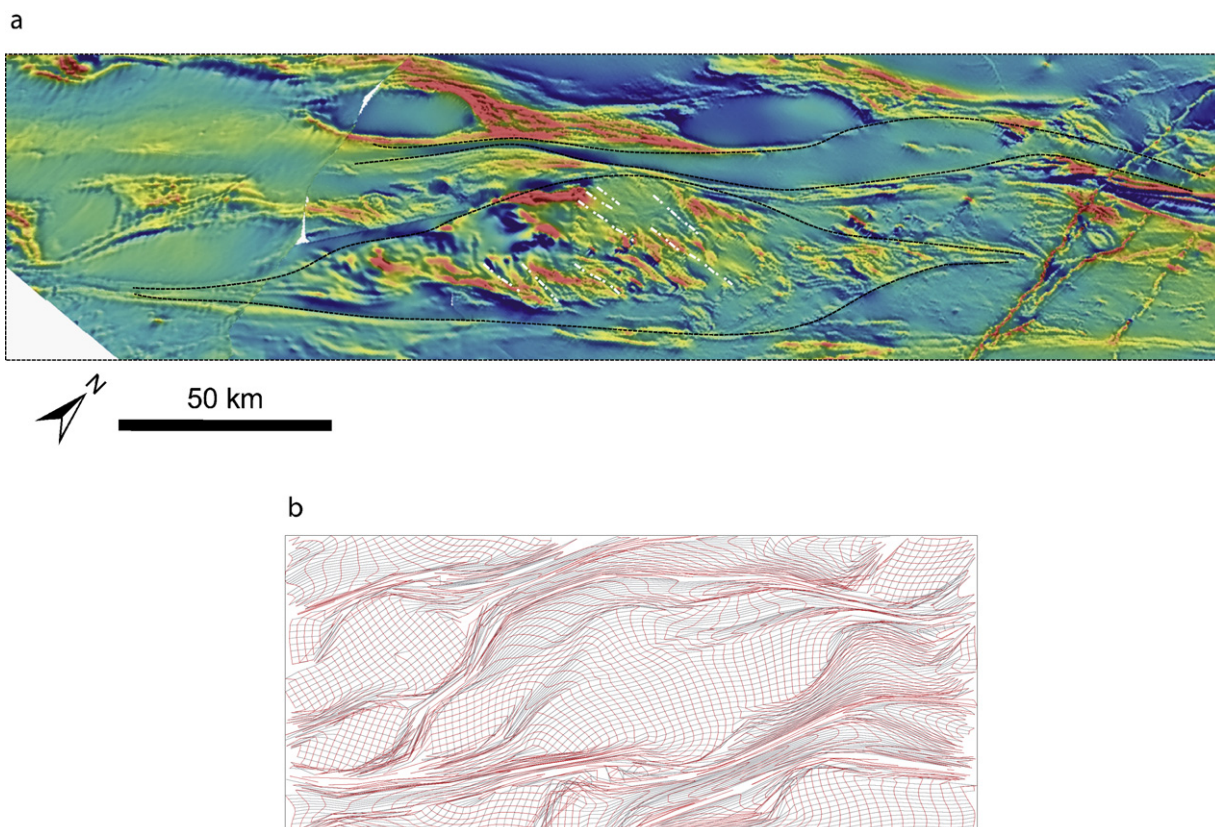
Fig. 12. Comparison between the overall magnetic fabric (annotated with black dashed lines) and the magnetic foliations (annotated with white dashed lines) seen in the volcano-sedimentary sequences of the Sefwi Belt and adjacent sedimentary basin and deformed originally orthogonal grids (as for Fig. 7) of a mechanical model with 50% of the material with high and low viscosities ($\gamma = 4$, viscosity ratio = 10, stress exponent = 3, EVR = 46). Location of this image is shown as inset in Fig. 5.

Trouw, 2005). Without detailed mapping of the microstructures around one of the leucogranites, which is difficult if not impossible given the outcrop conditions, we leave the resolution of this question to a future date.

The partitioning of deformation between pure shear and simple shear domains seen in the numerical models would translate in the context of the flat-lying Comoé Basin sediments into domains of upright folding and thrusting versus vertical shear zones, respectively. This partitioning raises a more general question about structural analysis that uses differences in deformation geometry to differentiate phases of deformation, which is beyond the scope of this study. In their study of strain partitioning in the Mauritanides of NE Senegal, Dabo et al. (2008) suggest a two-stage history to explain the different deformation geometries that they observe. In the absence of absolute geochronological constraints, this work suggests that a single phase deformation history is an alternative possibility.

Our analysis suggests that overall the leucogranites have deformed internally in a relatively homogeneous fashion at the large scale, however the outcrop conditions in the study area are uniformly poor, and particularly poor in areas where the leucogranites themselves occur. As a result we cannot determine whether the large-scale homogeneity is the result of a finer scale heterogeneity, such as a series of conjugate shears. The homogeneous magnetic response of the leucogranites suggests that it may indeed be homogeneous at the smaller scale. The work of Metelka et al. (2011) has shown that the magnetic data is quite capable of showing the presence of finer scale shears seen in outcrop in deformed granites from Burkina Faso, such as the Gaoua Pluton (their Fig. 8a).

The patterns of magnetic foliations in the greenstones of the Sefwi Belt itself reflect the patterns seen in the basin sediments,

but suggest a more homogeneous response, except for two elongate tails of material that stretch out from each end of a more irregular grouping made up of several different lithologies. This pattern resembles those seen in our mechanical models where the area ratio of more and less viscous materials was 50% (Fig. 12). Interestingly, the EW magnetic foliation seen within the Sefwi Belt proper is subparallel to the orientation of grid lines in our mechanical models which were originally parallel to the bulk flow direction (NW in our case). It is thus conceivable, but obviously subject to further investigation, that this magnetic foliation reflects an originally NE–SW structural grain formed during an earlier deformation phase.

5.4. Reconstruction

If we accept the modest estimates for rheological contrast suggested by our mechanical modelling, we arrive at a shear strain of 5γ for the Sunyani-Comé region. The width of deformed sediments and greenstones between the Ketesso High Strain Zone and the most north-westerly of the deformed leucogranites is at least 80 km. Combining these two measurements gives a total displacement of 400 km, excluding any displacement on the Ketesso High Strain Zone itself. Assuming a dextral shear sense, this places the domain found South-East of the Sefwi Belt (what we might call EoGhana?) at a position prior to deformation 400 km to the NE of its current position, near the border with current day Niger (Fig. 13). If we are mistaken and the shear really is sinistral, this zone would be somewhere in modern-day Brazil prior to deformation. It may be possible to test these hypotheses by analyzing paleomagnetic data from the many granitoid plutons and mafic dyke suites that cross the area, if we can find a set that pre-dates the deformation (Nomade et al., 2003). This might also help to constrain the age of
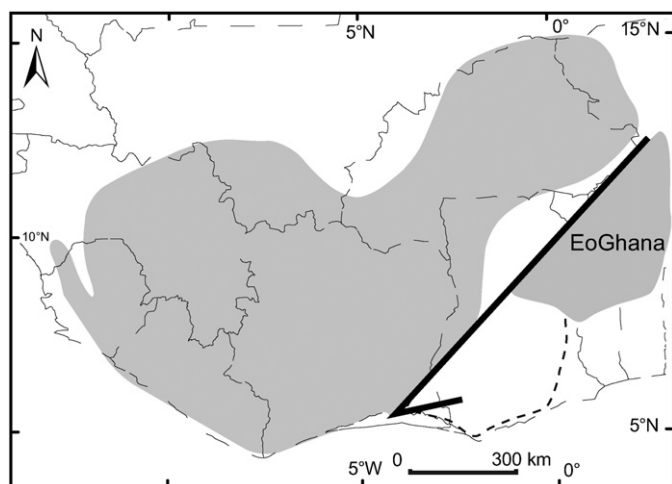
Fig. 13. Proposed reconstruction of the position of SW Ghana (EoGhana?) prior to the activity of the Sefwi shear system. Grey areas show Birimian and Archean terranes, dashed area shows present day location of Ghanaian Birimian terrane.

deformation itself, which we can bracket as being younger than the leucogranites (2081 Ma) and older than the formation of the Volta Basin (Neoproterozoic).

If we consider the Ketesso High Strain Zone, which in the field displays a strike-parallel mineral lineation which plunges between 5° and 10° to the SW (Hirdes et al., 2007), it will add another increment of displacement to our calculation, but since there are no markers that can be seen to be offset by this fault, the absolute value can only be estimated. To this end we can consider the total length of the fault zone, from the Atlantic coast to the loss of signal beneath the Volta Basin, which gives a strike length of over 500 km. Based on fault length-slip compilations, and admitting that this type of analysis is based on brittle structures (e.g. Scholz, 2002) this suggests a maximum displacement of around 50 km, considerably less than that for the distributed shearing we have documented. Delor et al. (1992) and Hirdes et al. (2007) characterise a major boundary between Kumasi-Afema basin and Sefwi volcano-plutonic belt rocks which are greenschist facies vs Sunyani-Comoé Basin rocks which are of upper-greenschist to amphibolites facies. Similarly, Feybesse et al. (2006) use contrasts in the metamorphic grade between the basins either side of the Sefwi Belt to infer that there is a significant shift in crustal level between the basins, which was due to the activity of reverse faults within the system. If we instead accept the estimate of a 50 km dextral displacement for the Ketesso High Strain Zone, with a slip vector plunging 5–10° to the SW (Hirdes et al., 2007), this equates to an uplift between 4 and 9 km for the NW region, which quite nicely accounts for the observed increase in the metamorphic grade across the Ketesso High Strain Zone (Galipp et al., 2003). Further uplift may be associated with the broader deformation zone in the Sunyani-Comoé Basin; however this would be marked by gradual change in metamorphic grade, and we would need to carry out systematic traverses to provide inputs to more detailed metamorphic analyses. If we look at the geological record of SE Burkina Faso, which we postulate was nearby to our EoGhana prior to the late shearing described here, we can see abundant evidence for dextral shearing (Ganne et al., 2012), which has been estimated based on the orientation of the lineation and the metamorphic grade contrast to be at least 50 km.

6. Conclusions

Based on mechanical modelling of two-phase systems coupled with an interpretation of the regional magnetic dataset, the Sunyani-Comoé Basin leucogranites show a viscosity contrast of approximately 7:1 between the leucogranites and their host sediments. This strongly suggests that the leucogranites had cooled prior to deformation, and were not synkinematic, but may still have been syntectonic.

An analysis of circularity versus orientation and circularity versus area shows that these leucogranites deformed in a dominantly simple shear environment, but that there was a strong partitioning of finite deformation and vorticity between the leucogranites and the sediments, and within the sediments themselves.

An estimated finite simple shear of 5γ combined with a deformation-zone width of 80 km gives a total horizontal displacement of 400 km across the zone, which for a dextral shear sense places SW Ghana prior to deformation at the level of current day southern Niger. This is in addition to an estimated 50 km of displacement on the Ketesso High Strain Zone.

Acknowledgements

References

Abouchami, W., Boher, M., Michard, A., Albarède, F., 1990. A major 2.1 Ga event of mafic magmatism in West Africa: an early stage of crustal accretion. Journal of Geophysical Research 95 (11), 17605–17629.

Adadey, K., Clarke, B., Théveniaut, H., Urien, P., Delor, C., Roig, J.Y., Feybesse. J.L., 2009. Geological Map Explanation—Map Sheet 0503 (1:100 000). Geological Survey Department Of Ghana (Gsd), No Mssp/2005/Gsd/5a.

Adou, M., Delor, C., Simeon, Y., Zamble, Z., Konan, G., Yao, B., Vidal, M., Diaby, I., Cautru, J.-P., Chiron, J.-C., Dommanget, A., Cocherie, A., 1995. Carte Géologique de la Côte d'Ivoire à 1/200 000, Feuille Abengourou. Direction de la Géologie, Abidjan, Côte d'Ivoire.

Agyei Duodu J., Loh G.K., Boamah K.O., Baba M., Hirdes W., Toloczyki M., Davis D.W., 2009. Geological Map of Ghana 1:1,000,000; Geological Survey of Ghana, Map 1:1 M.

Allibone, A., Hayden, P., Cameron, G., Duku, F., 2004. Paleoproterozoic gold deposits hosted by albite- and carbonate-altered tonalite in the Chirano District, Ghana, West Africa. Economic Geology and the Bulletin of the Society 99 (3), 479–497.

Allibone, A., Teasdale, J., Cameron, G., Etheridge, M., Uttley, P., Soboh, A., Appiah-Kubi, J., Adanu, A., Arthur, R., Mamphey, J., Odoom, B., Zuta, J., Tsikata, A., Pataye, F., Famiyeh, S., 2002a. Timing and structural controls on gold mineralization at the Bogoso gold mine, Ghana, West Africa. Economic Geology 97, 949–969.

Allibone, A.J., McCuaig, T.C., Harris, D., Etheridge, M., Munroe, S., Byrne, D., Amanor, J., Gyapong, W., 2002b. Structural controls on gold mineralization at the Ashanti Gold Mine, Obuassi, Ghana, vol. 9. Society of Economic Geologists Special Publication, pp. 65–93.

Ama Salah, L., Liegeois, J.-P., Pouclet, A., 1996. Evolution d'un arc insulaire océanique birimien précoce au Liptako nigérien (Sirba): géologie, géochronologie et géochimie. Journal of African Earth Sciences 22, 235–254.

Amponsah, P.O., 2012. Multiscale Structural Analysis of the Sunyani Basin, Ghana. Unpublished MSc Thesis, Department of Earth Science, University of Ghana, 107 pp.

Baratoux, L., Metelka, V., Naba, S., Jessell, M.W., Grégoire, M., Ganne, J., 2011. Juvenile Paleoproterozoic crust evolution during the Eburnean orogeny (~2.2–2.0 Ga), western Burkina Faso. Precambrian Research 191, 18–45.

Bell, T.H., 1981. Foliation development: the contribution, geometry and significance of progressive bulk inhomogeneous shortening. Tectonophysics 75, 273–296.

Bessoles, B., 1977. Géologie de l'Afrique. Le craton Ouest-Africain, Mémoires BRGM, Paris, p. 88.

Berthé, D., Choukroune, P., Jégouzo, P., 1979. Orthogneiss, mylonite and non coaxial deformation of granites—example of the South Armorican Shear Zone. Journal of Structural Geology 1, 31–42.

Béziat, D., Bourges, F., Debat, P., Lompo, M., Martin, F., Tollon, F., 2000. A Paleoproterozoic ultramafic-mafic assemblage and associated volcanic rocks of the Boromo greenstone belt: fractionates originating from island-arc volcanic activity in the West African craton. Precambrian Reserach 101, 25–47.

Blenkinsop, T., Schmidt Mumm, A., Kumi, R., Sangmor, S., 1994. Structural geology of the Ashanti gold mine. Geologisches Jahrbuch D 100, 131–153.

Boher, M., Michard, A., Albarede, F., Rossi, M., Milési, J.P., 1992. Crustal growth in West Africa at ca 2.1 Ga. Journal of Geophysical Research 97 (B1), 345–369.

Bonhomme, M., 1962. Contribution a l'étude géochronologique de la plate-forme de l'Ouest africain. Thesis, Ann. Fac. Sci. Univ. Clermont-Ferrand, Geol. Minéral. 5, 62 pp.

Bons, P.D., Koehn, D., Jessell, M.W., 2008. Microdynamics Simulation. Series: Lecture Notes in Earth Sciences, vol. 106, 406 pp. ISBN: 978-3-540-25522-255.

Bouchez, J.L., Delas, C., Gleizes, G., Nédélec, A., Cuney, M., 1992. Submagmatic microfractures in granites. Geology 20, 35–38.

Bourges, F., Debat, P., Tollon, F., Munoz, M., Ingles, J., 1998. The geology of the Taparko gold deposit, Birimian greenstone belt, Burkina Faso, West Africa. Mineralium Deposita 33, 591–605.

Castaing, C., Billa, M., Milési, J.P., Thiéblemont, D., Le Mentour, J., Egal, E., Donzeau, M., Guerrot, C., Cocherie, A., Chèvremont, P., Tegyey, M., Itard, Y., Zida, B., Ouedraogo, I., Kote, S., Kabore, B.E., Ouedraogo, C., Ki, J.C., Zunino, C., 2003. Notice explicative de la carte géologique et miniére du Burkina Faso à 1/1 000 000. BRGM, BUMIGEB, p. 147.

Dabo, M., Gueye, M., Ngom, P.M., Diagne, M., 2008. Orogen-parallel tectonic transport: transpression and strain partitioning in the Mauritanides of NE Senegal. In: Ennih, N., Liegeois, J.P. (Eds.), Boundaries of the West African Craton, vol. 297. Geological Society Special Publication, pp. 483–497.

Dampare, S.B., Shibata, T., Asiedu, D.K., Osae, S., Banoeng-Yakubo, B., 2008. Geochemistry of Paleoproterozoic metavolcanic rocks from the southern Ashanti volcanic belt, Ghana: Petrogenetic and tectonic setting implications. Precambrian Research 162, 403–423.

Davis, D.W., Hirdes, W., Schaltegger, E., Nunoo, E.A., 1994. U/Pb age constraints on deposition and provenance of Birimian and goldbearing Tarkwaian sediments in Ghana, West Africa. Precambrian Research 67, 89–107.

Debacker, T.N., Sintubin, M., 2008. The Quenast plug: a mega-porphyroclast during the Brabantian Orogeny (Senne valley, Brabant Massif). Geologica Belgica 11, 199–216.

Debat, P., Nikiema, S., Mercier, A., Lompo, M., Beziat, D., Bourges, F., Roddaz, M., Salvi, S., Tollon, F., Wenmenga, U., 2003. A new metamorphic constraint for the Eburnean orogeny from Paleoproterozoic formations of the Man shield (Aribinda and Tampelga countries, Burkina Faso). Precambrian Research 123, 47–65.

Dell'Angelo, L.N., Tullis, J., 1988. Experimental deformation of partially melted granitic aggregates. Journal of Metamorphic Geology 6, 495–515.

Delor, C., Diaby, I., Simeon, Y., Adou, M., Zamble, Z., Tastet, J.-P., Yao, B., Konan, G., Chiron, J.-C., Dommanget, A., 1992. Carte Géologique de la Côte d'Ivoire à 1/200 000, Feuille Grand-Bassam. Direction de la Géologie, Abidjan, Côte d'Ivoire.

Doumbia, S., Pouclet, A., Kouamelan, A., Peucat, J.P., Vidal, M., Delor, C., 1998. Petrogenesis of juvenile-type Birimian (Paleoproterozoic) granitoids in Central Côte-d'Ivoire, West-Africa: geochemistry and geochronology. Precambrian Research 87, 33–63.

Dunnet, D., 1969. A technique of finite strain analysis using elliptical particles. Tectonophysics 7, 117–136.

Eshelby, J.D., 1957. The Determination of the Elastic Field of an Ellipsoidal Inclusion, and Related Problems. Proceedings of the Royal Society of London. Series A, Mathematical and Physical Sciences 241, 376–439.

Feybesse, J.L., Billa, M., Guerrot, C., Duguey, E., Lescuyer, J.-L., Milési, J.-P., Bouchot, V., 2006. The Paleoproterozoic Ghanaian province: geodynamic model and ore controls, including regional stress modeling. Precambrian Research 149, 149–196.

Galipp, K., Klemd, R., Hirdes, W., 2003. Metamorphism and geochemistry of the paleoproterozoic Birimian volcanic Sefwi Belt (Ghana, West Africa). Geologisches Jahrbuch D 111, 151–191.

Ganne, J., De Andrade, V., Weinberg, R., Vidal, O., Dubacq, B., Kagambega, N., Naba, S., Baratoux, L., Jessell, M.W., Allibon, J., 2012. Modern-style plate subduction preserved in the Palaeoproterozoic West African Craton. Nature Geosciences, http://dx.doi.org/10.1038/ngeo1321.

Gapais, D., 1989. Shear structures within deformed granites: mechanical and thermal indicators. Geology 17, 1144–1147.

Gasquet, D., Barbey, P., Adou, M., Paquette, J.L., 2003. Structure, Sr–Nd isotope geochemistry and zircon U–Pb geochronology of the granitoïds of Dabakala area (Côte d'Ivoire): evidence for a 2.3 Ga crustal growth event in the Paleoproterozoic of West Africa? Precambrian Research 127, 329–354.

Glazner, A.F., John, M., Bartley, J.M., Coleman, D.S., Gray, W., Taylor, R.Z., 2004. Are plutons assembled over millions of years by amalgamation from small magma chambers? GSA Today 14 (4/5), 4–11.

Gumiaux, C., Gapais, D., Brun, J.P., Chantraine, J., Ruffet, G., 2004. Tectonic history of the Hercynian Armorican Shear belt (Brittany, France). Geodinamica Acta 17, 289–307.

Hein, K.A.A., 2010. Succession of structural events in the Goren greenstone belt (Burkina Faso): implications for West African tectonics. Journal of African Earth Sciences 56, 83–94.

Hirdes, W., Davis, D.W., 1998. First U–Pb zircon age of extrusive volcanism in the Birimian Supergroup of Ghana/West Africa. Journal of African Earth Sciences 27, 291–294.

Hirdes, W., Davis, D.W., Eisenlohr, B.N., 1992. Reassessment of Proterozoic granitoid ages in Ghana on the basis of U/Pb zircon and monazite dating. Precambrian Research 56, 89–96.

Hirdes, W., Davis, D.W., Ludtke, G., Konan, G., 1996. Two generations of Birimian (Paleoproterozoic) volcanic belts in northeastern Cote d'Ivoire (West Africa): consequences for the 'Birimian controversy'. Precambrian Research 80, 173–191.

Hirdes, W., Konan, K.G., N'Da, D., Okou, A., Sea, P., Zamble, Z.B., Davis, D.W., 2007. Geology of the Northern Portion of the Oboisso Area, Côte d'Ivoire. Sheets 4A, 4B, 4B BIS, 4. Direction de la Géologie, Abidjan, Côte d'Ivoire and Bundesanstalt für Geowissenschaften und Rohstoffe, Hanover.

Houseman, G., Barr, T., Evans, L., 2008. Basil: stress and deformation in a viscous material. In: Bons, P.D., Koehn, D., Jessell, M.W. (Eds.), Microdynamics Simulation. Lecture Notes in Earth Sciences, vol. 106. Springer, Berlin, p. 405.

Jessell, M.W., Bons, P.D., Evans, L., Barr, T., Stuwe, K., 2001. Elle: the numerical simulation of metamorphic and deformation microstructures. Computers & Geosciences 27 (1), 17–30.

Jessell, M.W., Bons, P.D., Griera, A., Evans, L., Wilson, C.J.L., 2009. A tale of two viscosities. Journal of Structural Geology, http://dx.doi.org/10.1016/j.jsg.2009.04.010.

Jessell, M.W., Santoul, J., Baratoux, L., Rousse, S., Naba, S., 2010. A more complete database of West Africa mafic dykes, EGU General Assembly 2010. Vienna, http://meetingorganizer.copernicus.org/EGU2010/EGU2010-2226-2011.pdf (last accessed 14/12/2010).

John, T., Klemd, R., Hirdes, W., Loh, G., 1999. The metamorphic evolution of the paleoproterozoic (Birimian) volcanic Ashanti belt (Ghana, West Africa). Precambrian Research 98, 11–30.

Kenis, I., Urai, J.L., van der Zee, W., Hilgers, C., Sintubin, M., 2005. Rheology of fine grained siliciclastic rocks deforming in the middle crust. Earth and Planetary Science Letters 233, 351–360.

Kříbek, B., Sýkorová, I., Machovič, V., Laufek, F., 2008. Graphitization of organic matter and fluid-deposited graphite in Paleoproterozoic (Birimian) black shales of the Kaya-Goren greenstone belt (Burkina Faso, West Africa). Journal of Metamorphic Geology 26, 937–958.

Ledru, P., Pons, J., Milesi, J.P., Feybesse, J.L., Johan, V., 1991. Transcurrent tectonics and polycyclic evolution in the Lower Proterozoic of Senegal-Mali. Precambrian Research 50, 337–354.

Leube, A., Hirdes, W., Mauer, R., Kesse, G.O., 1990. The early Proterozoic Birimian Supergroup of Ghana and some aspects of its associated gold mineralization. Precambrian Research 46, 139–165.

Lira, C., Pina, P., 2009. Automated grain shape measurements applied to beach sands. Journal of Coastal Research, 1527–1531, Special Issue No. 56.

Lisle, R.J., 1977. Clastic grain shape and orientation in relation to cleavage from the Aberystwyth Grits, Wales. Tectonophysics 39, 381–385.

Lompo, M., 2010. Paleoproterozoic structural evolution of the Man-Leo Shield (West Africa). Key structures for vertical to transcurrent tectonics. Journal of African Earth Sciences 58, 19–36.

Lüdtke, G., Hirdes, W., Konan, G., Koné, Y., N'da, D., Traoré, Y., Zamblé, Z., 1999. Géologie de la région Haute Comoé Sud—feuilles Dabakala (2b, d et 4b, d), Direction de la Géologie Abidjan Bulletin, p. 176.

Lüdtke, G., Hirdes, W., Konan, G., Koné, Y., Yao, C., Diarra, S., Zamblé, Z., 1998. Géologie de la région Haute Comoé Nord—feuilles Kong (4b et 4d) et Téhini-Bouna (3a à 3d), Direction de la Géologie Abidjan Bulletin, p. 178.

Metelka, V., Baratoux, L., Naba, S., Jessell, M., 2011. A geophysically constrained lithostructural analysis of the Eburnean greenstone belts and associated granitoid domains, Burkina Faso, West Africa. Precambrian Research 190, 48–69.

Milési, J.P., Feybesse, J.L., Ledru, P., Dommanget, A., Ouedraogo, M.F., Marcoux, E., Prost, A., Vinchon, C., Sylvain, J.P., Johan, V., Tegyey, M., Calvez, J.Y., Lagny, P., 1989. Minéralisations aurifères de l'Afrique de l'ouest, leurs relations avec l'évolution litho-structurale au Protérozoïque inférieur. Carte géologique au 1/2.000.000. Chronique de la recherche minière 497, 3–98.

Milési, J.P., Feybesse, J.L., Pinna, P., Deschamps, Y., Kampunzu, H., Muhongo, S., Lescuyer, J.L., Le Goff, E., Delor, C., Billa, M., Ralay, F., Heinry, C., 2004. Geological map of Africa 1:10,000,000, SIGAfrique project. In: 20th Conference of African Geology, BRGM, Orléans, France, 2–7 June, http://www.sigafrique.net (last accessed 14/12/2010).

Milési, J.P., Ledru, P., Feybesse, J.L., Dommanget, A., Marcoux, E., 1992. Early Proterozoic ore deposits and tectonics of the Birimian orogenic belt, West Africa. Precambrian Research 58, 305–344.

Naba, S., Lompo, M., Debat, P., Bouchez, J.L., Béziat, D., 2004. Structure and emplacement model for late-orogenic Paleoproterozoic granitoids: the Tenkodogo-Yamba elongate pluton (Eastern Burkina Faso). Journal of African Earth Sciences 38, 41–57.

Niederkorn, R., Blumenfeld, P., 1989. FUSION: a computer simulation of melting in the quartz-albite-anorthite-orthoclase system. Computers & Geosciences 15, 347–369.

Nikiéma, S., Benkhelil, J., Corsini, M., Bourges, F., Abdoulaye, D., Maurin, J.-C., 1993. Tectonique transcurrente éburnéenne au sein du craton ouest-africain: exemple du sillon de Djibo (Burkina Faso). Comptes Rendus de l'Academie des Sciences 316, 661–668.

Nomade, S., Chen, Y., Pouclet, A., Féraud, G., Théveniaut, H., Daouda, B.-Y., Vidal, M., Rigolet, C., 2003. The Guiana and the West African Shield Palaeoproterozoic grouping: new palaeomagnetic data for French Guiana and the Ivory Coast. Geophysical Journal International 154, 677–694.

Oberthür, T., Vetter, U., Davis, D.W., Amanor, J.A., 1998. Age constraints on gold mineralization and paleoproterozoic crustal evolution in the Ashanti belt of southern Ghana. Precambrian Research 89, 129–143.

Passchier, C.W., Trouw, R.A.J., 2005. Microtectonics. Springer, Berlin, 366 pp.

Pons, J., Barbey, P., Dupuis, D., Léger, J.M., 1995. Mechanisms of pluton emplacement and structural evolution of a 2.1 Ga juvenile continental crust: the Birimian of southwestern Niger. Precambrian Research 70, 281–301.

Pons, J., Oudin, C., Valéro, J., 1992. Kinematics of large syn-orogenic intrusions: example of the Lower Proterozoic Saraya batholith (Eastern Sénégal). Geologische Rundschau 82 (2), 473–486.

Pouclet, A., Vidal, M., Delor, C., Siméon, Y., Alric, G., 1996. Le volcanisme bir-
  imien du nord-est de la Côte-d'Ivoire, mise en évidence de deux phases
  volcano-tectoniques distinctes dans l'évolution géodynamique du Paléopro-
  térozoïque. Le Bulletin de la Société géologique de France 167 (4), 529–541.
Ramsay, J.G., 1967. Folding and Fracturing of Rocks. McGraw-Hill, New York, 531 pp.
Roman-Berdiel, T., Gapais, D., Brun, J.-P., 1997. Granite intrusion along strike-
  slip zones in experiment and nature. American Journal of Science 297,
  651–678.
Rosenberg, C.L., Handy, M.R., 2005. Experimental deformation of partially melted
  granite revisited: implications for the continental crust. Journal of Metamorphic
  Geology 23, 19–28.
Scholz, C.H., 2002. The Mechanics of Earthquakes and Faulting, 2nd ed. Cambridge
  Univ. Press, Cambridge.
Sestini, G., 1973. Sedimentology of a Paleoplacer: the Gold-bearing Tarkwaian of
  Ghana. International Union of Geological Sciences. Series A 3, 275–305.
Siegfried, P., De Kock, G.S., Clarke, B., Agenbacht, A., Delor, C., Van Rooyen, R.C., 2009.
  Geological Map Explanation—Map Sheet 0903D (1:100 000), Mining Sector Sup-
  port Programme. CGS, BRGM, Geoman, GSD, Accra.
Simeon. Y., Oelor. C., Oiaby, I., Gaoou, G., Kohou, P., Tastet, J.-P., Yao, B., Konan G.,
  Oommanget, A., 1992. Carte Géologique de la Côte d'Ivoire à 1/200 000; Feuille
  ABIDJAN, Direction de la Géologie. Abidjan. COte d'Ivoire.
Taylor, P.N., Moorbath, S., Leube, A., Hirdes, W., 1992. Early Proterozoic crustal evo-
  lution in the birimian of Ghana: constraints from geochronology and isotope
  geochemistry. Precambrian Research 56, 97–111.
Thomas, E., De Kock, G.S., Baglow, N., Viljoen, J.H.A., Z., S., 2009. Geological Map
  Explanation—Map Sheet 0903B (1:100,000), Mining Sector Support Programme.
  CGS, BRGM, Geoman, GSD, Accra.
Truffert, C., Gumiaux, C., Chantraine, J., Perrin, J., Galdeano, A., Gapais, D., Ballèvre,
  M., Asfirane, F., Guennoc, P., Brun, J.P., 2001. Levé géophysique aéroporté dans
  le Sud-Est du Massif armoricain (programme GéoFrance 3D Armor 2). In: Mag-
  nétisme et radiométrie spectrale, vol. 333. Comptes Rendus de l'Académie des
  Sciences, Paris, pp. 263–270.
Tullis, J., Yund, R.A., 1977. Experimental Deformation of Dry Westerly Granite. Jour-
  nal of Geophysical Research 82, 5705–5718.
Vidal, M., Gumiaux, C., Cagnard, F., Pouclet, A., Ouattara, G., Pichon, M., 2009. Evolu-
  tion of a Paleoproterozoic weak type orogeny in the West African Craton (Ivory
  Coast). Tectonophysics 477, 145–159.
Whitelaw, O.A.L., 1929. The geological and mining features of the Tarkwa-Abosso
  Goldfield. Gold Coast Geological Survey: Memoir 1, 1–45.
Yao, B.-D., Delor, C., Simeon,Y., Diaby, I., Gadou, G., Kohou, P., Okou, A., Konate, S.,
  Konan, G., Vidal, M., Cocherie, A., Dommanget, A., Cautru J.-P., Chiron, J.-C., 1995.
  Carte Géologique de la Côte d'Ivoire à 1/200 000; Feuille DIMBOKRO, Direction
  des Mines et de la Géologie, Abidjan, Côte d'Ivoire.
Zunic, J., Hirota, K., 2008. Measuring shape circularity. In: Ruiz-Schulcloper,
  J., Kroptasch, W. (Eds.), Progress in Pattern Recognition, Image Anal-
  ysis and Applications—LNCS, vol. 5197. Springer, Berlin, Germany,
  pp. 94–101.